Effect of Size, Surface Charge, and Hydrophobicity on the Translocation of Polystyrene Microspheres Through Gastrointestinal Mucin

DANIEL A. NORRIS, PATRICK J. SINKO

College of Pharmacy, Rutgers, The State University of New Jersey, P.O. Box 789, Frelinghuysen Road, Piscataway, New Jersey 08855

Received 27 March 1996; accepted 13 June 1996

ABSTRACT: Microspheres (MS) have been proposed for use as oral vaccine delivery vehicles (VDV); however, due to poor and variable absorption their clinical utility is limited. The effects of size, ζ-potential, and surface hydrophobicity on the translocation (P_T) permeabilities of polystyrene (PS) MS with varying surface functional groups (amidine, carboxyl, carboxylate-modified [CML], and sulfate) were determined through gastrointestinal (GI) mucin. P_T were determined, under steady-state conditions, using a modified Ussing-type diffusion chamber and a mucin packet developed for use with the Transwell-Snapwell system. P_T followed the Stokes–Einstein relationship, demonstrating the limited ability of larger MS (>0.5 μm) to diffuse through the mucin layer. P_T also varied according to the surface characteristics. Even though the ζ-potential did not correlate with the transport of MS through mucin, surface ionization appears to be important in MS translocation. The PS–amidine MS were significantly less hydrophobic and had a higher P_T than that of the other MS, suggesting that hydrophobicity is also a significant factor in MS transport through mucin. While these results suggest that mucin may be a significant barrier to the oral absorption of vaccines and VDVs *in vivo,* the rate-limiting barrier for the absorption of MS will be the intestinal mucosa. © 1997 John Wiley & Sons, Inc. J Appl Polym Sci **63:** 1481–1492, 1997

Key words: mucin; polystyrene microspheres; hydrophobicity; surface modification; intestinal transport

INTRODUCTION

The weak immunogenicity, low intestinal permeability, and high presystemic clearance of vaccines from the gastrointestinal (GI) tract requires the use of prohibitively large and repetitive doses to elicit even a modest immune response[1] making mass immunization programs economically unfeasible. Controlled-release polymeric microspheres (MS) have exhibited considerable potential as vaccine delivery vehicles (VDVs).[2–6] Ideally, VDVs must protect the immunogen from GI inactivation, promote transport through biological barriers such as mucin and the intestinal mucosa, augment the immune response, and control the kinetics of vaccine presentation to antigen presenting cells (APCs) thereby promoting an effective immune response.

The intestine not only allows for the absorption of nutrients, electrolytes, and fluid, but also acts as a barrier to prevent the free mixing of toxic lumenal contents with the underlying interstitial and vascular fluids, thus preventing the absorption of potentially harmful substances. For VDVs to be absorbed, they must pass through two barri-

Correspondence to: P. J. Sinko

Contract grant sponsors: Associated Institutes of Materials Science; Corning-CoStar Corp.

ers that are in series: the mucosa and the mucus gel layer. The mucosal tissue acts as a barrier since it restricts the penetration of vaccines, even though it is an incomplete barrier to macromolecules and particulate materials. Vaccine components may enter the intestinal mucosa at several possible sites, including the tips of villi where enterocytes are extruded, across or between enterocytes, or by specialized epithelial tissue composed of membraneous (M) cells that cover lymphoid aggregates known as Peyer's Patches.[7,8]

Intestinal mucus, a high molecular weight glycoprotein secretion, covers the mucosa with a continuous adherent blanket. The primary function of the mucus layer is to protect the gastrointestinal mucosa from potentially harmful bacteria, pathogens, or chemicals.[9–11] Several investigators have shown that mucin significantly decreases the diffusion of small and large compounds such as bovine serum albumin (BSA),[12] lysozyme,[12] tertiary amines, quaternary ammonium compounds,[13] and others.[14] The thickness of the mucin gel layer varies regionally throughout the GI tract with thickness decreasing distally from 50 to 500 μm (Ref. 10) in the stomach to 16–150 μm (Refs. 15–17) in the colon. The primary gel-forming component of the mucus layer is mucin, a highly heterogeneous glycoprotein, composed of a protein backbone to which carbohydrate side chains of various lengths are O-linked to serine or threonine amino acid residues[11] which form a mucin subunit. Several subunits joined by disulfide bonds form mucin molecules as large as 2×10^6 D. The concentration of mucin in the mucus gel layer also varies regionally. The concentration of mucin is reported to be $\sim$ 50, $\sim$ 40, $\sim$ 30, and $\sim$ 20 mg/mL in the stomach, duodenum, jejunum-ileum, and colon, respectively.[11,17,18]

In this report, an Ussing-type diffusion chamber system was developed to investigate the barrier properties of mucin using model VDVs composed of polystyrene (PS). The permeability of PS MS of varying size and surface properties were determined and correlations were established demonstrating that the mucus layer may be a significant barrier to the intestinal absorption of VDVs.

EXPERIMENTAL

Materials

PS MS of various sizes (0.5 μm yellow-green/amidine surface, 1.0 μm red/carboxyl surface, 0.01, 0.1, 0.2, 0.5, 1.0, and 2.0 μm yellow-green/carboxylate-modified [CML], and 0.5 μm yellow-green/sulfate surface) were purchased from Molecular Probes (Eugene, OR). Nucleopore polycarbonate filters were purchased from Corning-Costar Corp. (Cambridge, MA). All other materials were purchased from either Sigma Chemical (St. Louis, MO) or Fisher Scientific (Springfield, NJ) and used as received.

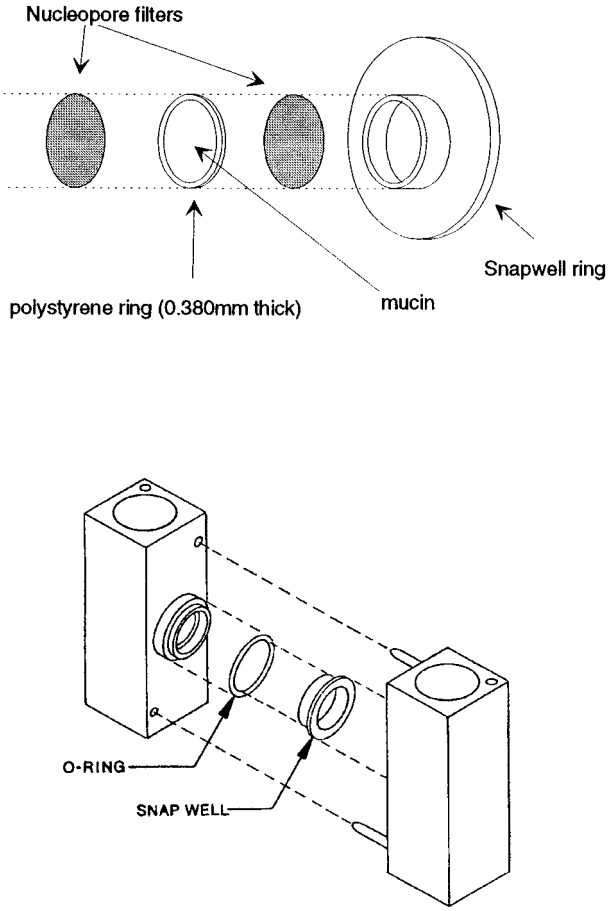

Figure 1 Modifications to Snapwell ring and schematic of Transwell-Snapwell diffusion chambers. The 0.4 μm filter supplied with Snapwell rings is removed and mucin is placed between two polycarbonate filters of appropriate size (see text). Snapwell fits within the diffusion chamber and is sealed in place with rubber O-rings.

Modifications to Ussing-type Diffusion Chambers

Ussing-type diffusion chambers (Corning-Costar Corp.) were used with modified Snapwell rings to maintain a vertical layer of mucin (Fig. 1). The original filters were removed with a scalpel and

replaced with Nucleopore polycarbonate filters of varying pore sizes using a cyanoacrylate adhesive. A polystyrene plastic ring approximately 0.38 mm thick was then glued onto the Snapwell ring. The modified Snapwell was filled with 50 μL of reconstituted mucin (20, 30, or 50 mg/mL) and then sealed with a second filter.

Mucin was prepared by reconstituting gastric mucin (porcine, crude type II, Sigma Chemical Co.). Mucin was mixed with sodium phosphate/sodium carbonate buffer (pH 6.5) in a mortar and triturated until completely wetted. The gel was then diluted to the appropriate concentration (20–50 mg/mL) and mixed well. Mucins from all mammalian species, including human and porcine mucins, share considerable structural similarities.[9–11] Included in these shared properties are the molecular weight and rheological properties for native and reconstituted, purified mucins from gastric and small intestinal regions.[19–21]

Diffusion Chamber System Validation

The barrier properties of the mucin packet were validated prior to the initiation of the uptake and translocation experiments in order to confirm the integrity of the system during the time course of the experiment. Three studies were performed: the loss of mucin from the packet during the experiment, the ability of the mucin packet to maintain an ionic (pH) gradient, and the binding of the MS to the chamber components.

Loss of Mucin from the Packet During the Experiment

The modified Snapwell rings were placed within diffusion chambers and both sides (donor and receptor) of the chamber were filled with 7 mL 0.01*M* sodium phosphate/sodium carbonate buffer at pH 6.5. The chambers were placed in prewarmed heating blocks and the gas lift system connected. The gas lift system continuously bubbles 95% O_2 : 5% CO_2 into each half-chamber to provide mixing during the experiment. After 90 min at 37°C, the concentration of mucin within the packet was determined using an established method based on a periodic acid/Schiff base reaction.[22] The loss of mucin was evaluated using the filters with pore sizes of 1, 2, 3, 5, 8, and 10 μm and physiologically relevant mucin concentrations 20, 30, and 50 mg/mL.[17]

Table I Polystyrene Microsphere Concentrations in Donor Chamber

Microsphere Surface[a]	Particle Diameter (μm)	Donor Concentration (particles/mL)
Sulfate	1.0	5.0×10^7
Amidine	0.5	1.0×10^8
Carboxyl	1.0	5.0×10^7
CML	0.01	1.0×10^{13}
CML	0.1	2.25×10^{10}
CML	0.2	1.8×10^9
CML	0.5	6.5×10^8
CML	1.0	5.0×10^7
CML	2.0	2.5×10^6

[a] Amidine = amide group; CML = carboxylate-modified.

The Ability of the Mucin Packet to Maintain an Ionic (pH) Gradient

The donor chamber was filled with buffer at pH 6.5 and the receptor chamber with buffer at pH 7.4 with the mucin layer mounted between the two half-chambers. The pH was then measured on both sides of the diffusion chamber for 90 min using a Ag/AgCl electrode.

Molecular Weight Distribution of Mucin

Size-exclusion chromatography was used to characterize the molecular weight distribution of reconstituted mucin. A low-pressure glass chromatography column (1.5 cm i.d.) was filled to a height of 50 cm with Sepharose 2B size exclusion media. One milliliter of mucin (1 mg/mL) was added to the column and eluted with a mobile phase consisting of 0.2% NaCl and 0.02% sodium azide as a preservative. The mobile phase was pumped at a flow rate of 0.2 mL/min using a peristaltic pump and 2 mL fractions were collected and assayed for mucin. Chromatograms were generated to determine the molecular weight distributions for two mucin concentrations (50 and 30 mg/mL) at pH 6.5 and 2.5.

The Binding of MS to the Chamber Components

The binding of MS to the acrylic chamber was determined by filling both sides of the diffusion chambers with the MS suspension. The concentrations used are given in Table I. Smaller MS are less fluorescent than are larger MS and therefore require higher concentrations to produce detectable levels during analysis. Samples were re-

moved at 0, 5, 10, 15, 30, and 60 min and assayed using a Shimadzu RF-5000 spectroflourophotometer. Yellow/green fluorescent MS were assayed at excitation λ = 490 nm and emission λ = 510 nm. Red fluorescent MS were assayed at excitation λ = 585 nm and emission at λ = 610 nm.

To correct for MS binding to the receptor chamber, an empirical correction factor was determined. MS of known concentration, equal to the expected amount transported, were added to the receptor chamber every 2 min. Samples were collected from the receptor chamber and assayed at 30, 60, 90, and 120 min. These concentrations were then compared to the amount of MS added to the chamber. The empirical correction factor was calculated by the following general equation:

$$ECF(MS, time) = \frac{C_{\text{theoretical}}}{C_{\text{experimental}}} \qquad (1)$$

where ECF is the empirical correction factor which is a function of both the MS and the sample time, $C_{\text{theoretical}}$ is the concentration of MS added to the chamber, and $C_{\text{experimental}}$ is the experimentally determined MS concentration at each time point. The ECF was multiplied by the experimentally determined transport concentrations to determine the actual amount of MS which transported within each time point.

Microsphere Surface Characterization

Zeta Potential

The ζ-potential was determined at pH values ranging between 2.0 and 10.0 using a BI-Zeta Plus (Brookhaven Instrument Corp.). MS were diluted to a concentration of 0.002% solids in 0.001*M* sodium phosphate/sodium carbonate buffer; the pH was adjusted using 0.01*N* HCl or 0.01*N* sodium hydroxide.

Confirmation of Particle Size

The particle-size range was confirmed using a BI-Zeta Plus instrument. MS suspensions (2% solids) were diluted 2 μL to 3 mL in 0.01*M* sodium phosphate/sodium carbonate buffer (pH 6.5). The particle size was measured for 2 min, five times for each MS. All cuvettes and solutions were rinsed and/or filtered to remove dust prior to measurement. The agglomeration of MS was determined by diluting MS suspensions (2% solids) to the concentrations shown in Table I using sodium phosphate/sodium carbonate buffer (pH 6.5) and measuring the particle size for 90 min at 37°C. No agglomeration, as indicated by an increase in effective particle size with time, was observed for any MS during the experiment.

Hydrophobic Interaction Chromatography (HIC)

The relative hydrophobicity of PS MS was determined using hydrophobic interaction chromatography based on a previously described method.[23] Briefly, columns were prepared using Pasteur pipettes (5 $\frac{3}{4}$ in. $L \times \frac{1}{4}$ in. i.d.) containing a small amount of glass wool with ethyl, pentyl, hexyl, or octyl agarose beads by gravity feed to a column height of 3 cm (1.2 mL of agarose suspension). The columns were then washed with at least 10 mL of 0.6*M* NaCl buffered to pH 7.4 with 0.001*M* sodium phosphate to remove the residual suspending solvents. One hundred microliters of microsphere suspension (0.02% solids) were added to the top of the column and eluted by gravity flow with 5 mL 0.6*M* NaCl followed immediately by 5 mL of 0.1% Triton X-100. The eluate was collected and assayed for MS. HIC was performed eight times for each surface.

Contact Angle

Two milligrams of MS, suspended in water, were cast onto a microscope slide and evaporated to dryness. The MS were scraped off the slide, collected, and dissolved in 1 mL of xylenes (mixture of *o*-, *m*-, and *p*-xylene). The polymer solution was then cast onto a coverslip and the solvent evaporated to dryness to obtain a smooth film. The contact angle was then determined using distilled water and a Rame-Hart NRL Model 100 goniometer. Ten measurements were made on each cast film.

Microsphere Transport

Snapwell rings were prepared as described to contain mucin at 30 mg/mL. The Snapwell rings were inserted into the diffusion chambers which were then placed in heating blocks prewarmed to 37°C. MS suspensions were added to the donor side and blank buffer was added to the receptor side. The donor concentrations used are shown in Table I. Diffusion chambers were removed serially every 30 min for 2 h. The mucin layer was completely removed and diluted to 3 mL in sodium phosphate buffer. Since mucin did not fluoresce at the wave-

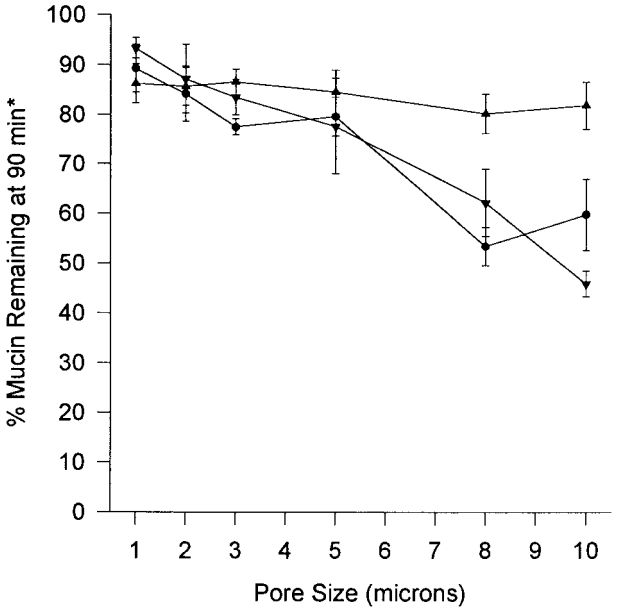

Figure 2 The percent mucin remaining within the packets after 90 min, 37°C, pH 6.5. Mucin packets were prepared containing (▲) 50 mg/mL mucin, (▼) 30 mg/mL mucin, and (●) 20 mg/mL mucin placed between polycarbonate filters of varying pore size.

lengths used, corrections for background fluorescence were not necessary. The donor chamber was removed and refilled with a fresh MS suspension to maintain a constant donor chamber concentration every 30 min. The samples were assayed as previously described.

The translocation permeability, P_T, was calculated using the equation

$$P_T = \frac{V_R}{AC_0}\frac{dC_R}{dt} \qquad (2)$$

where dC_R/dt is the slope of the regression line of the receptor concentration vs. time plot; A, the surface area of the mucin layer (1.03 cm^2); C_0, the donor concentration of MS; and V_R, the volume of the receptor chamber (7 mL).

Nonlinear Regression Methods

Scientist for Windows (MicroMath Scientific Software, Salt Lake City, UT) was used to fit the experimental data to the Stokes–Einstein equation by nonlinear regression. P_T values were weighted by 1/SEM. The point at which the second derivative of the fitted curve approached zero was used as the size cutoff for MS transport through mucin.

Statistical Methods

Statistical analyses were performed using BMDP New System (BMDP Statistical Software, Los Angeles, CA). All values are reported as mean ± SEM. Differences are considered to be significant at $\alpha = 0.05$. A least significant difference test was performed to determine specific differences between means on any ANOVA with $\alpha < 0.05$.

RESULTS

Diffusion Chamber System Validation

The results of the validation studies are shown in Figures 2–4. The three concentrations of mucin evaluated in these studies (20, 30, and 50 mg/mL) correspond to the physiological concentrations of mucin found in the colon, jejunum-ileum, and stomach, respectively.[11,17,18] Filters with pore sizes less than 5 μm retained at least 85% of the mucin for 90 min for all three initial mucin concentrations (Fig. 2). When the pore size of the filter was greater than 5 μm, a significant amount

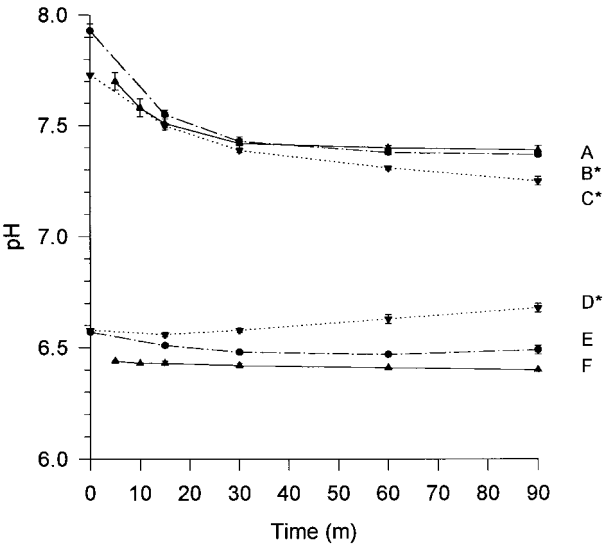

Figure 3 Maintenance of a barrier to pH by mucin packet. pH remains constant beginning at 30 min when H^+ diffusion between donor and receptor chambers is prohibited by a physical barrier: (▲) line A donor side, line F receptor side). pH changes significantly when donor and receptor chambers are separated by a packet containing buffer: (▼) line C donor side, line D receptor side. pH remains constant when donor and receptor chambers are separated by a mucin packet: (●) line B donor side, line E receptor side). (*) indicates slope is significantly different from 0 between 30 and 90 min.

of mucin diffused out of the packet (Fig. 2). Based on these results, all subsequent experiments were conducted with filters possessing pore sizes less than or equal to 5 μm. A mucin concentration of 30 mg/mL was utilized in order to simulate intestinal mucin concentrations.

The ability of the mucin layer to maintain an ionic gradient is shown in Figure 3. The mucin layer maintained a pH gradient between pH 6.5 and 7.4 better than the control (buffer placed between the filters) during the time course of the experiment.

To characterize potential structural changes in mucin during the time course of the experiment, size exclusion chromatography (SEC) was performed. Analysis of mucin composition was performed prior to and after completing the experiment. Typical chromatograms are shown in Figure 4. At pH 6.5, the amount of mucin (initial = 20, 30, and 50 mg/mL) retained in the 5 μm filter insert was approximately 85% (only 50 mg/mL data shown). The molecular size range of the retained mucin after the experiment [Fig. 4(b)] was found to be similar to control chromatograms [Fig. 4(a)], indicating that mucin loss was not attributable to a particular molecular weight fraction. The total mucin lost is consistent with that reported in Figure 2.

The binding of MS to the diffusion chambers [Fig. 5(a)] was dependent upon size. Over 90 min, 40–70% of the MS remained suspended in the diffusion chambers. To properly determine the steady-state translocation permeability using Fick's Law, it was necessary to maintain a constant donor MS concentration. To overcome this problem, 4 mL were removed from the donor chamber and replaced with 4 mL of fresh MS suspension. As shown in Figure 5(b), using this method, the concentration of MS in the donor chamber at 90 min was constant and not significantly different from the initial concentrations.

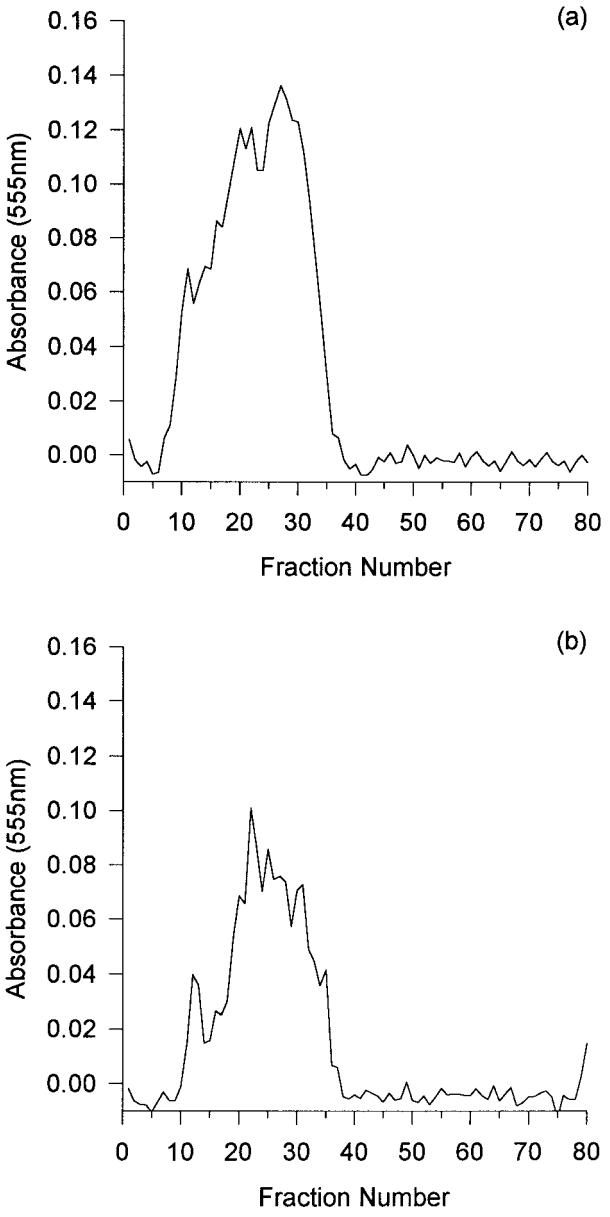

Figure 4 Size exclusion chromatograms for mucin reconstituted at 50 mg/mL: (a) mucin before diffusion experiment; (b) mucin retained within packet after a diffusion experiment. One milligram of mucin was added to a 50 cm Sepharose 2B column and eluted with 0.2% NaCl/0.02% sodium azide at a flow rate of 0.2 mL/min. Two milliliter fractions were collected and analyzed by periodic acid/Schiff base assay.

Microsphere Surface Characterization

Zeta (ζ)-Potential

The zeta (ζ)-potential is the potential difference between the charge on a surface and the bulk of the solution in which it is submerged. The values obtained for ζ-potential are dependent upon the ionic strength and pH of the buffer as well as upon the temperature at which the measurement is taken. The pH–ζ-potential profiles were characterized for the four MS surfaces (amidine, carboxyl, CML, and sulfate) studied and are shown in Figure 6. The positively charged surface, amidine, had less negative ζ-potential values compared to the other MS surfaces. The carboxylate-modified surface exhibited a moderately charged surface at pH values $>$ 6 when compared to the

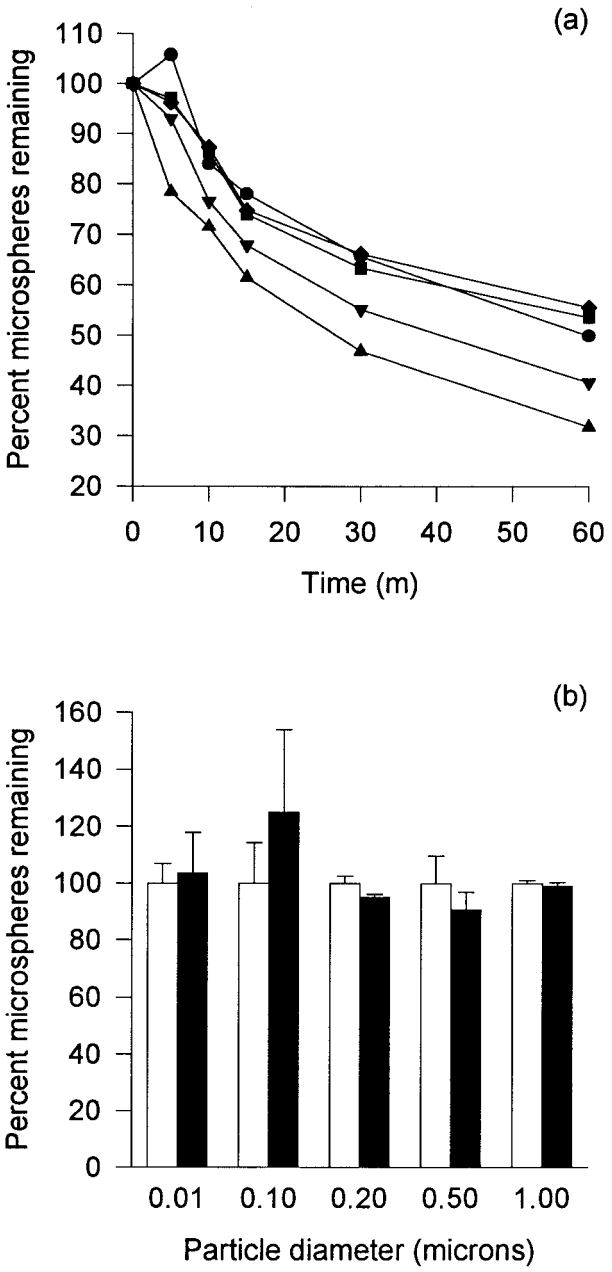

Figure 5 (a) The binding of MS to diffusion chambers over time, pH 6.5, 37°C: (▲) 0.01 μm; (▼) 0.1 μm; (●) 0.2 μm; (■) 0.5 μm; (♦) 1.0 μm. (b) Donor chamber concentrations using donor suspension replacement: (white) percent of initial concentration at t = 0 min, (black) percent of initial concentration at t = 90 min, pH 6.5, 37°C.

other surfaces. Using these pH profiles, it was possible to estimate the approximate pK_a value for each surface. The carboxyl and sulfate surfaces demonstrated a reduction in ζ-potential at 3.5 and 5.0, respectively, while the carboxylate-modified surface appeared to have a much lower pK_a ($\sim$ 2.5). A pK_a of 6.0 was estimated for the amidine surface.

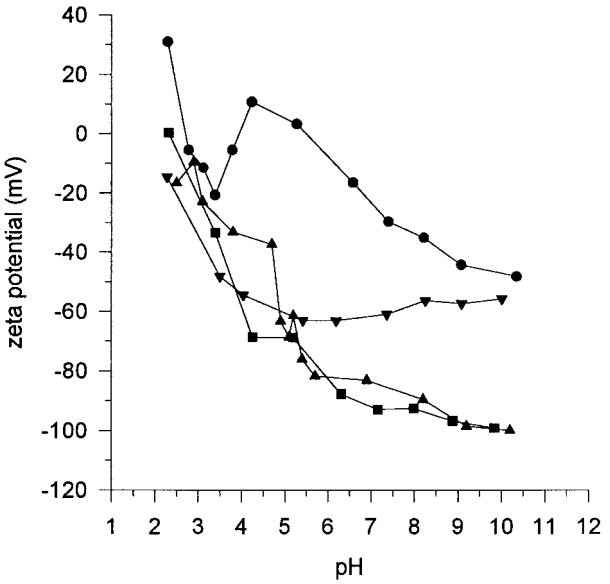

Figure 6 ζ-Potential of unmodified PS MS (0.002% solids) diluted in 0.001M sodium chloride/sodium carbonate buffer (ionic strength = 0.007) determined by laser light scattering using a BI-ZetaPlus instrument. Electrical field applied and reversed five times: (▲) PS–sulfate; (●) PS–amidine; (■) PS–carboxyl; (▼) PS–CML.

Contact Angle

The distilled water contact angle gives an indication of the hydrophobicity of the cast film. The results of the contact angle measurements are shown in Table II and Figure 7. Using this method, differences in contact angles could not be discerned. It is hypothesized that, by dissolving the MS in mixed xylenes before casting the films,

Table II Contact Angles and Hydrophobic Interaction Chromatography Results

Polystyrene Microsphere Surface[a]	Contact Angle (°)	HIC % Retained, Pentyl Agarose
Sulfate	71.3 ± 0.61	85.91 ± 6.19
Amidine	70.6 ± 1.95	70.42 ± 9.17[b]
Carboxyl	73.7 ± 0.75	93.66 ± 0.34
CML	73.5 ± 5.02	91.93 ± 2.33

[a] Amidine = amide group; CML = carboxylate-modified.
[b] Indicates statistical significance, P value $<.05$ after ANOVA followed by least significant difference analysis.

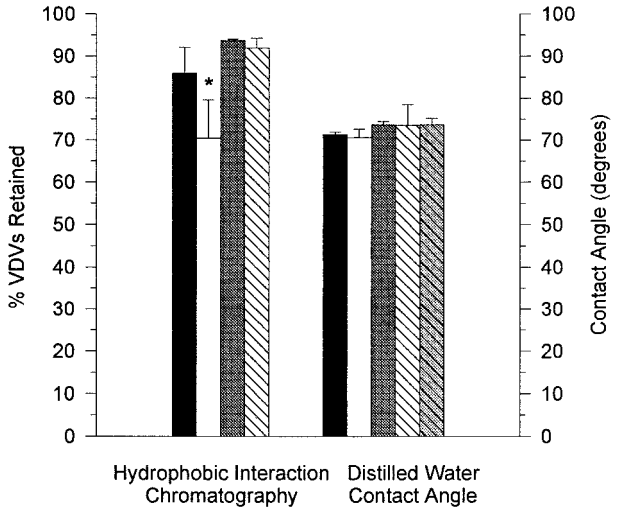

Figure 7 Percent MS retained on pentyl-agarose hydrophobic interaction chromatography columns ($5\ \frac{3}{4} \times \frac{1}{4}$ in.) eluted with 0.6*M* NaCl followed by 0.1% Triton X-100. Distilled water contact angle on cast films of MS dissolved in xylenes, 10 measurements, five on left side of sessile drops, five on right side. (Black) PS–sulfate; (white) PS–amidine; (gray) PS–carboxyl; (white-striped) PS–CML; (gray-striped) unformulated PS. (*) Percent PS–amidine on HIC only significant difference after ANOVA and least significant difference analysis.

the surface character of the MS was apparently abolished since only the surface groups of the MS were functionalized. Therefore, by dissolving the MS and casting a film, a significantly higher fraction of unfunctionalized PS was exposed on the surface of the film. As seen in Figure 7, the cast films' hydrophobicities are not significantly different than the control (nonfunctionalized PS) supporting this hypothesis.

Hydrophobic Interaction Chromatography (HIC)

Hydrophobic interaction chromatography allows the hydrophobicity of the MS to be evaluated without physically modifying the MS. Greater MS hydrophobicity will increase the percent of MS retained on the column. Preliminary experiments determined that the pentyl agarose media was the most efficient for detecting hydrophobic differences between the MS (data not shown). The HIC results run on pentyl agarose media are shown in Table II. Significant differences in the percent MS retained were found between the surfaces. The least retained MS were the amidine (70%). The percent of amidine MS retained was also significantly different from the percents retained for the sulfate (85%), carboxyl (93%), and CML MSs (91%). The HIC results are shown in Figure 7.

Microsphere Translocation

The calculated translocation permeabilities, P_T, for MS of different surfaces with similar size are shown in Table III and Figure 8. Significant differences in the calculated P_T of the MS were observed. The P_T of the PS–amidine MS was an order of magnitude greater than was the P_T for the other surfaces (5.36×10^{-4} vs. $\sim 3 \times 10^{-5}$ cm/min). The P_T for the PS–CML MS was 2.63×10^{-5} cm/min. The P_T for the PS–sulfate and PS–carboxyl MS were, respectively, 30 and 110% higher than the P_T for the PS–CML MS but were not significantly different due to the variability in the measurements.

The diffusion of particles through mucin should follow the Stokes–Einstein equation:

$$D = \frac{kT}{6\eta\pi r} \tag{3}$$

where k is the Boltzmann constant; T, absolute temperature; η, the viscosity of the medium; and

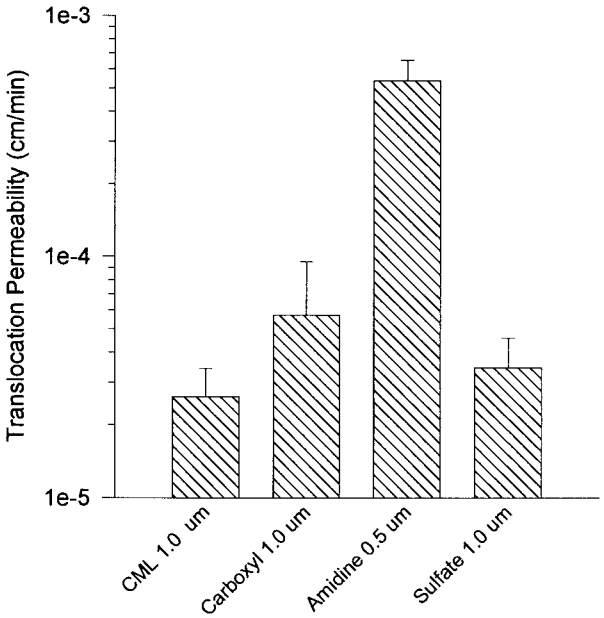

Figure 8 Translocation permeabilities for PS MS. Translocation permeabilities calculated by eq. (2) (see text). Permeabilities were determined through mucin packets containing mucin at 30 mg/mL and polycarbonate filters with 5 μm pores, pH 6.5 donor and 7.4 receptor, 37°C.

Table III Translocation Permeabilities

Polystyrene Microsphere Surface[a]	Reported Diameter (μm)	Actual Diameter (μm)	P_T (cm/min)
Sulfate	1.0	1.08	$3.46 \times 10^{-5} \pm 1.15 \times 10^{-5}$
Amidine	0.5	0.88	$5.36 \times 10^{-4} \pm 1.15 \times 10^{-5}$
Carboxyl	1.0	1.12	$5.54 \times 10^{-5} \pm 3.83 \times 10^{-5}$
CML	0.01	0.07	$2.54 \times 10^{-4} \pm 3.83 \times 10^{-5}$
CML	0.1	0.14	$1.11 \times 10^{-4} \pm 6.47 \times 10^{-5}$
CML	0.2	0.27	$4.57 \times 10^{-5} \pm 1.62 \times 10^{-5}$
CML	0.5	0.49	$7.85 \times 10^{-6} \pm 6.93 \times 10^{-6}$
CML	0.5	0.58	$1.06 \times 10^{-5} \pm 3.60 \times 10^{-6}$
CML	1.0	1.07	$2.63 \times 10^{-5} \pm 8.31 \times 10^{-6}$

[a] Amidine = amide group; CML = carboxylate-modified.

r, the radius of the diffusing particle. Since P (permeability) is equal to D/h, where D is the aqueous diffusion coefficient (cm^2/s) and h is the length of the diffusion pathway, the Stokes–Einstein equation can be rewritten as

$$P = \frac{kT}{6\eta\pi rh} \tag{4}$$

The translocation permeabilities (P_T) for five different sizes of CML MS were determined. For these studies, all MS had CML surface functional groups and the size was varied from 0.1 to 1 μm. The results are shown in Figure 9. Since the permeability coefficient, P, is directly proportional to D, by the equation $P = D/h$, and the diffusing particles are spherical, the translocation permeability should also follow the Stokes–Einstein equation. The translocation permeabilities were fitted to the Stokes–Einstein equation. This is shown in Figure 9 and demonstrated the limited ability of MS larger than 0.5 μm to diffuse through the mucin layer. These results indicate a sharp decrease in P_T as the MS diameter increases to approximately 0.3 μm. A gradual decrease is then observed as the diameter is increased to 0.5 μm where no further significant decrease in P_T is observed as the diameter increases. At MS diameters greater than 0.5 μm, the second derivative of the fitted curve approaches zero, which suggests a size range cutoff for MS larger than 0.5 μm. Figure 10 shows P_T plotted as a function of the hydrophobicity of the MS. The amidine MS, which have the highest P_T, also have the lowest hydrophobicity. The sulfate, CML, and carboxyl MS, which were retained equally on the pentyl agarose column, also show similar P_T.

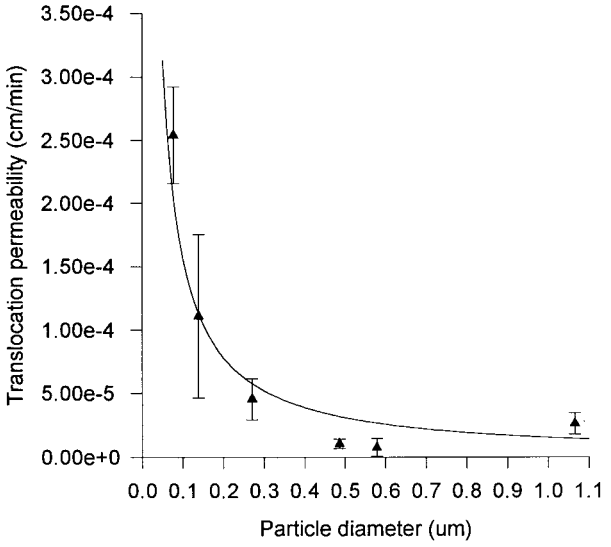

Figure 9 Translocation permeability of PS MS as a function of particle size. Translocation permeabilities calculated by eq. (2). Permeabilities were determined through mucin packets containing mucin at 30 mg/mL and polycarbonate filters with 5 μm pores, pH 6.5 donor and 7.4 receptor, 37°C. Curve was fitted to eq. (4), weighted by 1/SEM.

As shown in Figure 11, the ζ-potential at $\sim$ pH 7.0 vs. P_T shows that the ζ-potential may be a valuable indicator in determining the P_T. The highest P_T was associated with the MS that had the most positive ζ-potential (PS–amidine). For the other MS, the P_T gradually decreased as the ζ-potential became more positive.

DISCUSSION

It is well established that the major component of the mucus gel layer coating the intestinal membranes is mucin, a highly heterogeneous glycoprotein of molecular weight $1–2 \times 10^6$ D.[10,11] The

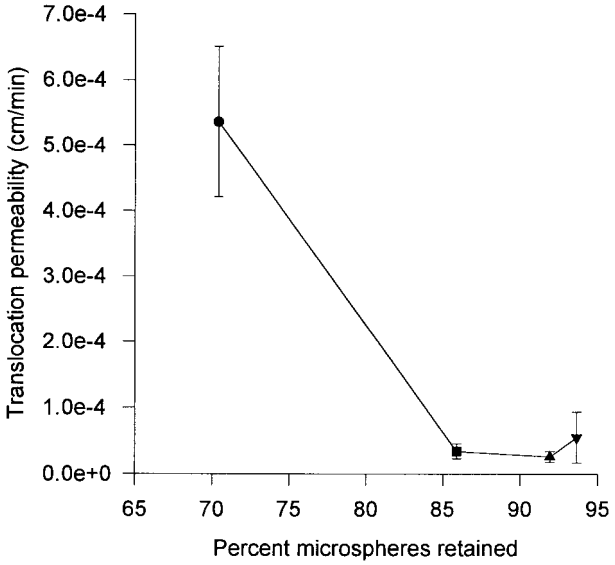

Figure 10 Correlation of translocation permeabilities in Figure 8 to percent MS retained on pentylagarose media (Fig. 7): (●) PS–amidine; (■) PS–sulfate; (▲) PS–CML; (▼) PS–carboxyl.

viscoelastic and gel-forming properties of purified mucin are comparable to native mucus gels.[17,18] Intestinal mucus functions as a barrier maintaining a pH difference between the GI lumen and the mucosal surface.[19–21] The role of mucus in drug and vaccine absorption from the GI tract has not been extensively studied. It was the objective of this investigation to determine the importance of mucus as a barrier to vaccine and microparticle absorption. Three fundamental parameters were studied: microparticle size, surface charge, and surface hydrophobicity using commercially available PS MS.

MS with diameters as large as 10 μm are reported to be taken up into M-cells[3]; however, only MS less than 5 μm are reported to be transported out of the M-cell. VDVs between 1 and 10 μm are readily phagocytosed by APCs such as macrophages[24–28] with an optimal size less than 5 μm. As shown in Figure 9, the PS–CML MS P_T's followed the Stokes–Einstein relationship demonstrating the limited ability of MS larger than 0.5 μm to diffuse through the mucin layer. A similar phenomenon was demonstrated for the gastrointestinal absorption of various poly(ethylene glycol)s (PEGs) by Donovan et al. who showed that the percent absorption of PEG decreased to less than 2% as the molecular weight was increased to 1500 and remained constant for larger size PEG molecules.[29] Preliminary data in this laboratory indicate that the P_T for PEG-4000 through the intestinal mucosa is 8.58×10^{-5} cm/min.[30] Based on the work of Donovan et al., the P_T for the larger PS MS should be no greater than the permeability for PEG-4000. Therefore, the PS MS would have, at best, a P_T of 8.5×10^{-5} cm/min through intestinal tissue. The PS–CML MS P_T through mucin were fitted to eq. (4) and the P_T calculated for a molecule approximately the size of PEG-4000. The P_T was estimated to be 7.94×10^{-4} cm/min, which is 10 times greater than the P_T observed for PEG-4000 through intestinal tissue. This suggests that GI mucus may not be the rate-limiting barrier to the intestinal uptake of microparticles and that the target size of orally administered VDVs should be less than 1 μm.

The second factor investigated was surface charge. For these studies, the size of the MS were fixed at 1.0 μm or, for the PS–amidine surface, which was not commercially available at 1.0 μm, 0.5 μm particles were selected. Based on the Stokes–Einstein relationship, which demonstrated that the P_T for particles above 0.5 μm was relatively independent of size, the difference in size would not bias the results. The PS–carboxyl, –CML, and –sulfate surfaces are negatively charged MS, while the PS–amidine MS is positively charged. The oligosaccharides surrounding the mucin protein core contain high levels of five monosaccharides: fucose, galactose, *N*-acetylga-

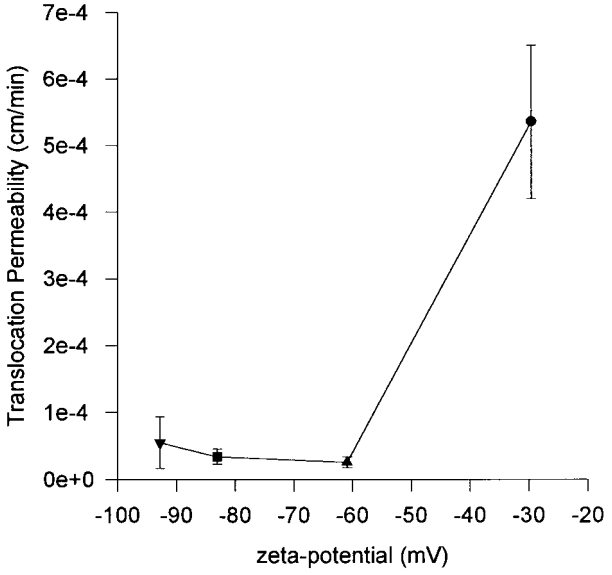

Figure 11 Correlation of translocation permeabilities in Figure 8 to ζ-potential (Fig. 6) at pH 7: (●) PS–amidine; (■) PS–sulfate; (▲) PS–CML; (▼) PS–carboxyl.

lactosamine, *N*-acetylglucosamine, and sialic acid.[11] These are neutral or negatively charged sugars which impart an overall negative charge to the mucin molecule. The MS can be ranked according to the P_T (PS–CML < PS–sulfate < PS–carboxyl ≪ PS–amidine). For the purpose of this discussion, the MS are placed into two groups: MS with relatively low P_T (PS–CML, PS–sulfate, and PS–carboxyl) and MS with relatively high P_T (PS–amidine). The pK_a values determined from Figure 6 indicate that the surface functional groups on PS–CML, PS–sulfate, and PS–carboxyl MS (low P_T) are almost completely ionized (>99%), while the surface of the PS–amidine MS (high P_T) is only 9% ionized. While it appears that there is a relationship between the surface ionization and P_T, further study is required to quantify these effects. The results shown in Figure 11 indicate that ζ-potential may not be a significant factor in determining the P_T of PS MS. On the one hand, since PS MS are significantly more hydrophobic than are other MS,[28] hydrophobic factors may have overwhelmed the effects of surface charge in the current study. On the other hand, Saitoh, et al.[13] showed that the charge of the species does not affect the diffusion of quaternary and tertiary amine compounds through mucin.

The third factor investigated was surface hydrophobicity. While literature reports concerning the hydrophobic effects on drug and vaccine transport through mucin are lacking, a considerable body of literature exists for bacteria. The interactions of potentially harmful pathogens such as *Yersinia enterocolitica, Escherichia coli,* and *Pseudomonas aeruginosa* with mucin have been determined to be hydrophobic in nature.[31–37] Although binding sites for *E. coli* have been found in mucin, the interaction is mediated through nonspecific hydrophobic interactions with the "link" glycoprotein.[36] In addition, the penetration of *Y. enterocolitica* through mucin depends upon the hydrophobicity of the surface.[35] The diffusion through mucin of strains grown with a more hydrophobic surface were inhibited while more hydrophilic strains penetrated much faster. Precoating of hydrophobic strains of *Y. enterocolitica* with mucin imparts a more hydrophilic surface, which, in turn, increased its transport through mucin, suggesting that hydrophobic interactions play an important role in the transport of bacteria through the mucus gel layer. The current results (Fig. 10) also suggest that an optimal hydrophobic/hydrophilic balance may be needed to facilitate the diffusion of MS through mucin since MS that were retained more than 85% on HIC were also less permeable.

The current results suggest that particle size, surface ionization, and surface hydrophobicity play an important role in the diffusion of model vaccine microparticles through GI mucus. Using a physiologically relevant mucin diffusion system, this investigation also demonstrated that mucin is expected to be a significant barrier in the oral absorption of vaccine microparticles; the mucin barrier, however, will only represent 10% or less of the total resistance to MS uptake.

An American Foundation for Pharmaceutical Education Fellowship and New Jersey Center for Biomaterials and Medical Devices Summer Fellowship (D.A.N.), the Hoechst Celanese Innovative Research Award (P.J.S.), the Associated Institutes of Materials Science, and Corning-CoStar Corp. are acknowledged for supporting these studies. The following are also gratefully acknowledged: Prof. Joachim Kohn (Department of Chemistry, Rutgers University) for the use of the goniometer used for contact angle measurements and Dr. Glen Leesman (Ribi ImmunoChem Research, Inc.) for performing the particle agglomeration studies.

REFERENCES

1. C. Czerkinsky, A. M. Svennerholm, and J. Holmgren, *Clin. Infect. Dis.,* **16,** S106–116 (1993).
2. R. Edelman, R. G. Russell, G. Losonsky, B. D. Tall, C. O. Tacket, M. M. Levine, and D. H. Lewis, *Vaccine,* **11,** 155–158 (1993).
3. J. H. Eldridge, C. J. Hammond, J. A. Meulbroek, J. K. Staas, R. M. Gilley, and T. R. Tice, *J. Contr. Rel.,* **11,** 205–214 (1990).
4. C. E. McQueen, E. C. Boedeker, R. Reid, D. Jarboe, M. Wolf, M. Le, and W. R. Brown, *Vaccine,* **11,** 201–206 (1993).
5. D. T. O'Hagan, J. P. McGee, J. Holmgren, A. M. Mowat, A. M. Donachie, K. H. G. Mills, W. Gaisford, D. Rahman, and S. J. Challacombe, *Vaccine,* **11,** 149–154 (1993).
6. R. H. Reid, E. C. Boedeker, C. E. McQueen, D. Davis, L. Y. Tseng, J. Kodak, K. Sau, C. L. Wilhelmsen, R. Nellore, P. Dalal, and H. R. Bhagat, *Vaccine,* **11,** 159–167 (1993).
7. R. L. Owen and A. L. Jones, *Gastroenterology,* **66,** 189–203 (1974).
8. J. L. Wolf and W. A. Bye, *Annu. Rev. Med.,* **35,** 95–112 (1984).
9. J. T. Lamont, *Ann. N.Y. Acad. Sci.,* **664,** 190–201 (1992).
10. M. R. Neutra and J. F. Forstner, in *Physiology of*

the Gastrointestinal Tract, L. R. Johnson, Ed., Raven Press, New York, 1987, pp. 975–1009.
11. G. J. Strous and J. Dekker, *Crit. Rev. Biochem. Mol. Biol.,* **27,** 57–92 (1992).
12. M. A. Desai, M. Mutlu, and P. Vadgama, *Experientia,* **48,** 22–26 (1992).
13. H. Saitoh, N. Hasegawa, S. Kawai, K. Miyazaki, and T. Arita, *J. Pharm. Dynam.,* **9,** 1008–1014 (1986).
14. M. A. Desai and P. Vadgama, *Analyst,* **116,** 1113–1116 (1991).
15. S. Kerss, A. Allen, and A. Garner, *Clin. Sci.,* **63,** 187–195 (1982).
16. T. Sakata and W. V. Engelhardt, *Cell Tiss. Res.,* **219,** 629–635 (1981).
17. L. A. Sellers, A. Allen, E. R. Morris, and S. B. Ross-Murphy, *Biorheology,* **24,** 615–623 (1987).
18. L. A. Sellers, A. Allen, E. R. Morris, and S. B. Ross-Murphy, *Carbohydr. Res.,* **178,** 93–110 (1988).
19. A. Allen, G. Flemstrom, A. Garner, and E. Kivilaakso, *Physiol. Rev.,* **73,** 823–857 (1993).
20. K. R. Bhaskar, P. Garik, B. S. Turner, J. D. Bradley, R. Bansil, H. E. Stanley, and J. T. Lamont, *Nature,* **360,** 458–461 (1992).
21. L. M. Lichtenberger, *Annu. Rev. Physiol.,* **57,** 565–583 (1995).
22. M. Mantle and A. Allen, *Biochem. Soc. Trans.,* **6,** 607–609 (1978).
23. C. J. Smyth, P. Jonsson, E. Olsson, O. Soderlind, J. Rosengren, S. Hjerten, and T. Wadstrom, *Infect. Immun.,* **22,** 462–472 (1978).
24. J. H. Eldridge, J. A. Meulbroek, J. K. Staas, T. R. Tice, and R. M. Gilley, *Adv. Exp. Med. Biol.,* **251,** 191–202 (1989).
25. S. M. Horowitz, C. G. Frondoza, and D. W. Lennox, *J. Orthop. Res.,* **6,** 827–832 (1988).
26. R. M. Steinman, I. S. Mellman, W. A. Muller, and Z. A. Cohn, *J. Cell Biol.,* **96,** 1–27 (1983).
27. Y. Tabata and Y. Ikada, *Biomaterials,* **9,** 356–362 (1988).
28. Y. Tabata and Y. Ikada, *J. Biomed. Mater. Res.,* **22,** 837–858 (1988).
29. M. D. Donovan, G. L. Flynn, and G. L. Amidon, *Pharm. Res.,* **7,** 863–868 (1990).
30. H. Yu, T. J. Cook, and P. J. Sinko, *Pharm. Res.,* **12,** S-304 (1995).
31. B. Drumm, A. W. Neumann, Z. Policova, and P. M. Sherman, *J. Clin. Invest.,* **84,** 1588–1594 (1989).
32. M. Mantle, L. Basaraba, S. C. Peacock, and D. G. Gall, *Infect. Immun.,* **57,** 3292–3299 (1989).
33. M. Mantle and S. D. Husar, *Infect. Immun.,* **61,** 2340–2346 (1993).
34. M. Mantle and S. D. Husar, *Infect. Immun.,* **62,** 1219–1227 (1994).
35. A. Paerregaard, F. Espersen, O. M. Jensen, and M. Skurnik, *Infect. Immun.,* **59,** 253–260 (1991).
36. S. U. Sajjan and J. F. Forstner, *Infect. Immun.,* **58,** 860–867 (1990).
37. U. Sajjan, J. Reisman, P. Doig, R. T. Irvin, G. Forstner, and J. Forstner, *J. Clin. Invest.,* **89,** 657–665 (1992).